JOURNAL OF Applied Polymer SCIENCE

Effects of Waste Ground Fluororubber Vulcanizate Powders on the Properties of Silicone Rubber/Fluororubber Blends

Dae Hyun Kim,[1] Sung Hyuk Hwang,[2] Tae Sung Park,[3] Bong Shik Kim[1]

[1]School of Chemical Engineering, Yeungnam University, Gyeongsan 712-749, Korea

[2]Sung Jong Company, Deagu University Business Incubating Center, Jillyang, Gyeongbuk 712-714, Korea

[3]Reliability Technology Center, Korea Institute of Footwear and Leather Technology, Busan, 614-100, Korea

Correspondence to: B. S. Kim (E-mail: kimbs@ynu.ac.kr)

ABSTRACT: We prepared fluororubber (FKM) vulcanizate powder (FVP) via cryogenic grinding of the FKM commonly used in automobiles and assessed the particle size distribution of the resulting powder. We also prepared silicone rubber (SR)/FKM blends at a ratio of 25/75. Varying amounts of FKM were replaced with equal amounts of FVP within the range of 5–40 wt%, and the physical properties of the resulting SR/FKM/FVP blends were investigated and compared. The TGA curves of the SR/FKM/FVP blends obtained during the thermal property investigations indicated that pyrolysis of SR occurred within two temperature ranges, and that the SR/FKM/FVP blends with 5 wt% FVP demonstrated the highest thermal stability. The storage modulus (E') and loss modulus (E'') of the SR/ FKM/FVP blends increased as the FVP content increased. In the SR/FKM/FVP blends with 5 and 10 wt% FVP, very typical elastic-deformation behavior was observed. On the contrary, in 40 wt% FVP, the rubber properties disappeared. The mean particle size of FVP was 41.75 μm, and particle size distribution measurements of the SR/FKM/FVP blends suggest particle coexistence such that FVP was condensed and separated. © 2012 Wiley Periodicals, Inc. J. Appl. Polym. Sci. 000: 000–000, 2012

KEYWORDS: blend; FVP; CGR; GTR; particle size

Received 20 September 2010; accepted 30 March 2012; published online
DOI: 10.1002/app.37822

INTRODUCTION

Waste rubber recycling is important for both environmental and economic reasons. Successful utilization of waste rubber in virgin rubber depends on the processing characteristics of the rubber compounds and the final properties of the resulting vulcanizates. The simplest approach to rubber recycling involves grinding of vulcanizates and utilization of the resulting powder. This method was first suggested by Charles Goodyear, who is also credited with the discovery of rubber vulcanization, in order to overcome the scarcity of natural rubber (NR).[1] Later, enterprising compounders found that they could selectively use the waste rubber dust obtained when rubber products are buffed to size as a compounding ingredient, resulting in reduced costs. This approach has the advantage of being environmentally friendly, involving no production of toxic gases or chemicals. Furthermore, the material value is not debased as it after pyrolysis or incineration. Therefore, the focus of several studies has been improvement of the cost effectiveness of this technique. Powdered rubber has been used to improve the impact strengths of plastics and the processabilities of rubber compounds and also for the production of thermoplastic elastomeric blends.[2] There are also reports on the preparation of products via vulcanization of natural rubber or styrene-butadiene rubber (SBR) lattices containing finely ground scrap tires and a large amount of mineral filler.[3] Powdered rubber is unique as a filler because of its large grain size (in the range of microns) and lower modulus compared to those of other commercial fillers used in the rubber industry. Like other fillers, the polarity (surface functional groups or the polar nature of the polymer) and the structure (spongy, chain-like aggregates or free-flowing powder) of ground vulcanizates affect the physicomechanical properties of ground rubber-filled vulcanizates.[4] When added to the same base compound (i.e., when the composition of the powdered rubber and the matrix are the same), powdered rubber can act as an extender to the rubber matrix, with minimal changes in the compound properties.

Luo and Isayev reported the development of composites based on ultrasonically devulcanized ground rubber tire (GRT) and polypropylene.[5] Adam et al. showed that the addition of 20 phr of polybutadiene rubber (BR) granulate grafted with

Table I. Blend Ratios of SR/FKM

Ingredients	A (phr)
SR[a]	25
FKM[b]	75
LS-4[c]	0.84
TAC 50%[d]	0.80

[a]Silicone rubber [KE941-U(SR)], [b]Fluororubber, [c]Peroxide (50% active content), [d]Triallylcyanurate (50% active content).

ethylacrylate to a polyacrylic rubber compound had deleterious effects on the physical properties of rubber.[6] Recently, Jacob et al. reported utilization of mechanically ground ethylene-propylene-diene monomer (EPDM) rubber vulcanizate as a filler in an EPDM compound.[7] While there have been several reports on the utilization of waste tire rubber,[8–16] reuse of waste specialty rubber has received less attention.

Blends of silicone rubber (SR) and fluororubber (FKM) are technologically compatible, as the SR forms a continuous phase and the FKM forms a dispersed phase.[17] The mechanical properties of the blends either follow the additive rule or show synergy, indicating cocrosslinking and consequent technological compatibility.

The 50/50 SR/FKM blend contains large, randomly distributed granules. The effects of replacement of the constituent rubbers in the 50/50 SR/FKM blend with the respective vulcanizate powders on the processability and mechanical properties of the resultant rubber compounds were studied by Ghosh et al.[17,18] SR is difficult to be prepared as a powder via cryogenic grinding because one advantage of SR has low temperature resistance.

Thereby, in this study, we prepared rubber vulcanizate powders via cryogenic grinding of FKM. The objective of this study was to investigate the recycling of rubber powder in detail. We hypothesized that virgin FKM can be successfully replaced with FKM vulcanizate powder (FVP) in the SR/FKM blends. We report the results of experimental investigations of the properties of 25/75 SR/FKM blend and of the partial replacement of virgin rubbers with ground FKM in the SR/FKM blends. We explored the effects of rubber recycling on the resulting physical properties including thermal properties, morphologies of the blends, and the particle size distribution of the FVP powder. Rubber vulcanizate powders were chosen as models for the corresponding waste rubbers.

EXPERIMENTAL

Materials

The poly(methylvinylsiloxane) (PMVS) or silicone rubber (SR) used in this study was of commercial grade (KE 941-U, hardness = 43 durometer A, plasticizing temperature = 190°C, tear strength = 15 kN m^{-1}, specific gravity = 1.11 g cm^{-3}, tensile strength = 6.5 MPa, elongation at break = 385%; Shin-Etsu, Japan). The vinylidene fluoride (VdF)/hexafluoroproplylene (HFP)/tetrafluoroethylene (TFE) terpolymers (FKM) used in our study were commercial grade elastomers (E-18894, specific gravity = 1.75, tensile strength = 16.5 MPa, elongation at break = 254%; Dyneon, USA). The crosslinking agent commercially known as LS-4 (2,5-bis-(*t*-butylperoxy)-2,5-dimethylhexane) was supplied by Dow Corning, Korea. The coagents were studied using triallylcyanurate (TAC: 2,4,6-triallyloxy-1,3,5-triazine, Aldrich, Korea).

Preparation of Samples

SR/FKM/FVP blends were prepared at a weight ratio of 25/75/0, 25/70/5, 25/65/10, 25/55/20, and 25/35/40. Rubber blends were prepared using an internal mixer (HAAKE, Rheocord 9000, Germany) at a rotor speed of 60 rpm at 80°C. FKM was first sheared for 5 min, and then SR was added in there and they were mixed for an additional 5 min. Finally, LS-4 and TAC were added in there and they were mixed for another 3 min. After mixing, the blends were formed into sheets in a two-roll open mixing mill at 60°C.

The optimum cure times of the compounds were measured with using a flat die rheometer (FDR). Rubber sheets of ~2 mm in thickness were prepared using a hot-press with a compression molder at 160°C and a pressure of 15 MPa for 20 min. Compounds used in this study are shown in Table I.

Preparation of Fluororubber Vulcanizate Powder

FVP was prepared according to the following procedure (also see Table II). First, FKM was sheared for 2 min in an internal mixer (HAAKE, Rheocord 9000, Germany) at 80°C and a rotor speed of 60 rpm. Then LS-4, coagent (TAC), and MT carbon black were added in there and they were mixed for 3 min. The blend was formed into sheets in a two-roll open mixing mill at 60°C. Thick sheets of ~2 mm were prepared via molding at 170°C for 20 min in a hot-press at a pressure of 15 MPa. Samples were then aged at 250°C for 24 h in an oven. Finally, FVP was prepared using a cryogenic sample crusher (Jai, JFC-300, Japan).

Samples of rubber (3 g) were put into sample vessels along with steel balls, and the sample vessels were placed into a crushing rod. Each sample vessel and crushing rod was shaken in liquid nitrogen with reciprocating movement at a speed of 1450 times per minute. Each sample was crushed completely by the steel balls, and the cryogenically crushed rubber was passed through a 50 mesh sieve and then a 325 mesh sieve.

Replacement of Virgin Fluororubber with FVP

Virgin FKM was replaced in SR/FKM/FVP blends with FVP according to the formulations given in Table III. First, FKM was sheared in an internal mixer (HAAKE, Rheocord 9000, Germany) for 2 min at 80°C and a rotor speed of 60 rpm. Then SR

Table II. Formulations of FKM

Ingredients	A (phr)
FKM	100
MT carbon black[a]	100
LS-4	2
TAC 50%	2.5

[a]MT carbon black (medium thermal black, N900).

Table III. Replacement of SR/FKM in 25/75 Blends with Vulcanizate Powder (FVP)

SR/FKM/FVP	A (phr)	B (phr)	C (phr)	D (phr)	E (phr)
SR	25	25	25	25	25
FKM	75	70	65	55	35
FVP[a]	–	5	10	20	40
LS-4	0.84	0.84	0.84	0.84	0.84
TAC 50%	0.80	0.80	0.80	0.8	0.80

[a]FVP (fluororubber vulcanizate powder).

Table IV. Curing Characteristics of SR/FKM/FVP Blends

SR/FKM/FVP	t_{min}[a]	t_{max}[b]	t_{10}[c]	t_{50}	t_{90}
25/75/0	0.62	6.16	1.13	2.73	5.91
25/70/5	0.77	6.42	0.99	5.32	11.63
25/65/10	0.80	6.14	1.02	5.32	11.71
25/55/20	1.03	8.32	1.04	5.22	11.32
25/35/40	1.83	14.65	1.04	3.68	7.76

[a]Minimum torque value (dN m), [b]Maximum torque value (dN m), [c]The time to 10% of the maximum torque value (min).

was added in there and they were mixed for 2 min, after which FVP was added in there. Finally, LS-4 and TAC were added in there and they were mixed for another 3 min. The hot material was formed into sheets in a two-roll mill.

Instrumentation

An internal mixer (HAAKE, Rheocord 9000, Germany) and two open mixing mills were used for mixing and blending. A hot-press was used for compression, heating, and crosslinking. The crosslinked blends were prepared under a pressure of 15 MPa for 20 min. To determine the curing behaviors of the blends, the cure characteristics of the compounds were determined using an Ueshma flat die rheometer (FDR, Japan) with 3 g samples of the blend compounds at 165°C for 30 min at an amplitude angle of 1°.

Thermogravimetric analysis (TGA) of samples were performed using a TA Instruments (TA Q 5000, USA) automatic programmer from a temperature of 800°C and increasing according to a programmed heating rate of 10°C min^{-1} in a platinum pan under nitrogen flow. A sample with a weight of ~30 mg was collected for each measurement. The degradation temperature (T_0) and the temperature of maximum weight loss (T_{max}) were evaluated for each sample.

Measurements of the dynamic mechanical properties of the blends were performed using a dynamic mechanical analyzer (DMA, RSA 3, TA Instruments, USA). The dual cantilever mode of the deformation geometer or the three-point bending mode was used in the range of −100 to 100°C at a heating rate of 10°C min^{-1} at a frequency of 10 Hz. The average specimen dimensions were 12 mm in length, 4 mm in width, and 3 mm in thickness. The storage modulus (E') and loss tangent (tan δ) were measured for all samples under identical conditions.

Stress–strain properties were measured according to ASTM D412-98 using a universal testing machine (Instron 5567, Germany). All tests were performed at −10, 25, and 80°C with a crosshead speed of 500 mm min^{-1}. The averages of five measurements were used to calculate the sample strengths.

Analyses of the particle size distributions of FVP were performed using a laser micron sizer (LMS 30, Japan). Before analyzing the particle size distributions, FVP particles were passed through a 50 and 325 mesh sieves. The ~3 g of powder was measured using a wet method with ethanol as the dispersion medium and a He-Ne gas laser ($\lambda = 0.6328$ μm). The particle size distributions were in the range of 0.1–1000 μm, with 55 channels. Only spherical particles were measured. While monitoring the particle diameter every 10 s, 10, 50, and 90% and the maximum of the particle diameter (defined as X_{10}, X_{50}, X_{90}, and X_{top}, respectively) in the volume standard cumulative distribution were measured under stabilized conditions.

The morphologies of the blends were investigated using field emission scanning electron microscopy (FE-SEM) with a Jeol

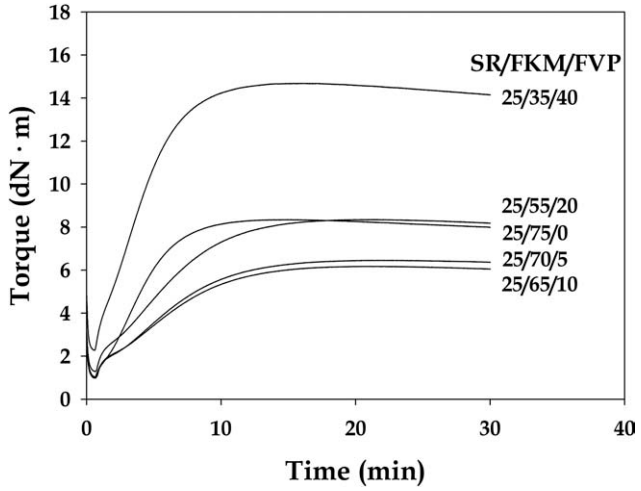

Figure 1. Curing characteristics of SR/FKM/FVP blends at 165°C.

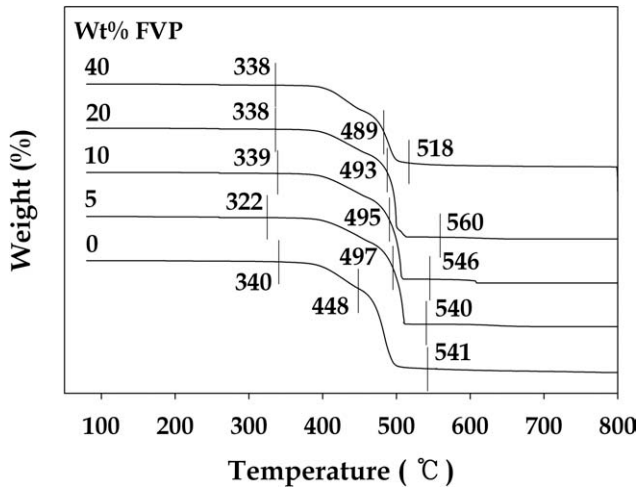

Figure 2. TGA curves of the SR/FKM/FVP blends.

Applied Polymer SCIENCE

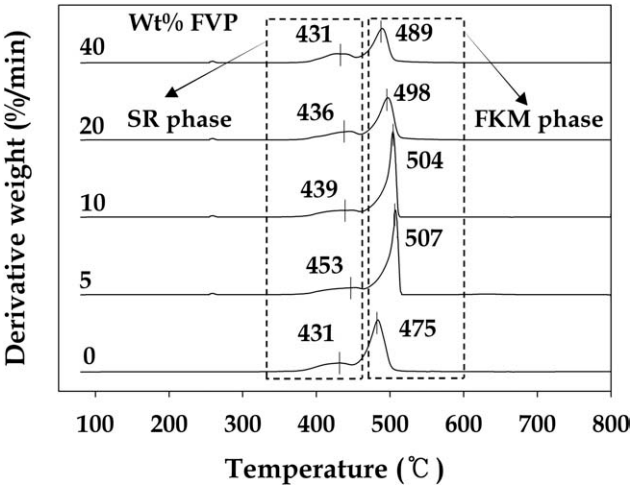

Figure 3. DTG curves of the SR/FKM/FVP blends.

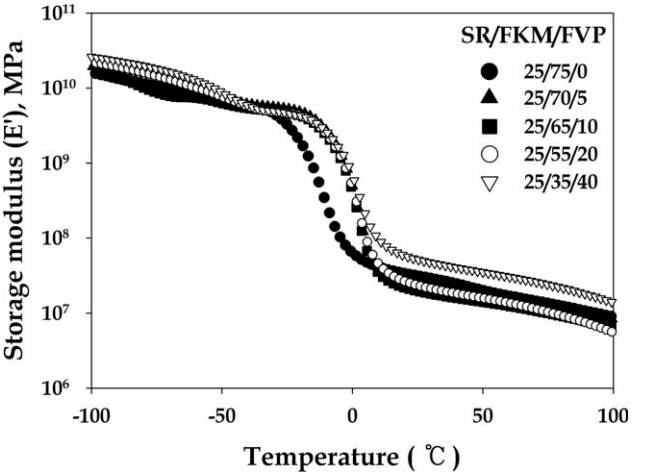

Figure 4. Storage modulus (E') of the SR/FKM/FVP blends.

instrument model JSM-6701F. Samples were fractured in liquid nitrogen and then coated with gold using a Cressington 108 auto sputter coater. The morphologies were evaluated at an accelerating voltage of 5 kV.

RESULTS AND DISCUSSION

The Cure Characteristics of the Blends

Five types of SR/FKM blends were prepared with different weight percentages in order to examine their cure characteristics. Figure 1 illustrates the method employed to record the curing characteristics using a rheometer with ASTM D 2084, and the results are presented in Table IV. The torque tended to increase with increasing curing time. The torque values of the 25/35/40 SR/FKM/FVP blend showed higher than that of the 25/75 SR/FKM blend. This is owing to the MT carbon black content included in FVP. Compared with that in the 25/35/40 SR/FKM/FVP blend, scorch time was more shorter in the 25/75 SR/FKM blend because the t_{90} was short. Carbon black is used to improve the physical properties of FKM with MT carbon black being particularly useful due to its physical stability.

The torque as a function of time, as shown in Figure 1, required periodic rotation to maintain a constant angle of a disk placed on the center of the rubber sheet. Given a specific type of power, the torque is proportional to the degree of curing and can be obtained using the following equation[19]:

$$\text{Degree of crosslinking (\%)} = \frac{T(t) - T_{\min}}{T_{\max} - T_{\min}} \times 100 \qquad (1)$$

where $T_{\max}$ is the value of the maximum torque (N· m), $T_{\min}$ is the value of the minimum torque, and $T(t)$ is the value of the torque at the cure time.

Thermal Properties

The thermal properties of the blends were evaluated using thermogravimetric analyzer (TGA) and derivative thermogravimetric (DTG) analyses were carried out between 80 and 800°C. Figures 2 and 3 show the TGA and DTG curves for all SR/FKM/FVP blends. The results are summarized in Table V.

The weight loss during the first stage is attributed to the loss of volatile products formed during the degradation process. The weight loss in the second stage is attributed to the formation of carbonaceous residue and silica filler.

In Figure 2, TGA curves of the 0, 5, 10, 20, and 40 FVP wt% exhibited a two-step thermal degradation. The first

Table V. Thermal Properties of Blends

SR/FKM/FVP	TGA temperature (°C) 1 wt% loss	DTG degradation wt % loss
25/75/0	340 (476)[a]	17.7[b] (66.6)[c]
25/70/5	322 (497)[a]	19.5[b] (75.9)[c]
25/65/10	339 (495)[a]	15.5[b] (75.9)[c]
25/55/20	338 (493)[a]	15.0[b] (65.8)[c]
25/35/40	338 (489)[a]	13.5[b] (53.9)[c]

[a]Temperature for 50% weight loss, [b]Wt% loss for the first thermal degradation, [c]Wt% loss for the second thermal degradation.

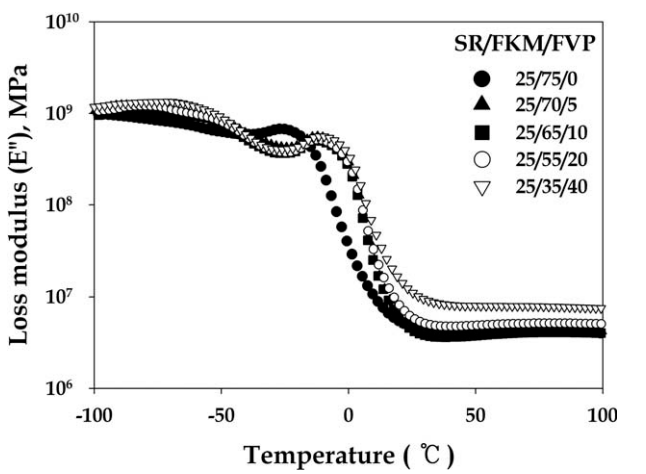

Figure 5. Loss modulus (E″) of the SR/FKM/FVP blends.

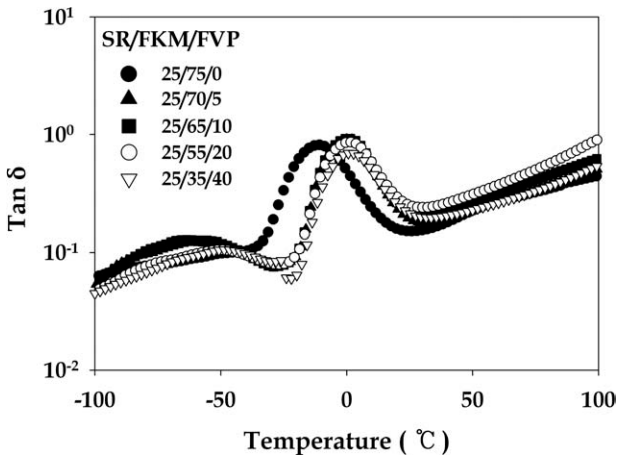

Figure 6. Tangent (tan δ) of the SR/FKM/FVP blends.

decomposition region of them occurred at 340–448°C, 322–497°C, 339–495°C, 338–493°C, and 338–489°C, respectively and the second region of them started at 448, 497, 495, 493, and 489°C and ends at 541, 540, 546, 560, and 518°C, respectively.

The significant increase in degradation temperature is probably due to the MT carbon black existing into the FVP. Thus, the SR/FKM/FVP blends had higher degradation temperatures than that of the SR/FKM blend. From Figure 2, the degradation temperatures of the 10, 20, and 40 wt% FVP blends were lower than those of the 25/70/5 SR/FKM/FVP blend. The marked differences in the thermal properties of these blends indicate that the filler–polymer interactions decreased with decreasing FKM content.[20,21]

The filler–polymer interactions lead to the formation of bound rubber by physical adsorption, chemical adsorption, and mechanical interaction. Factors affecting the formation of bound rubber have been studied by many researchers.[22–26] Bound rubber is a parameter that is simple to measure, although the factors which influence the test results are very complicated.

From Figure 2, the initial degradation temperature corresponding to 1% decomposition for the SR/FKM blend of 0, 5, 10, 20, and 40 wt% FVP were found to be 340, 322, 339, 338, and 338°C, respectively. With increasing FVP content, the SR/FKM/FVP blends showed a tendency toward decreased thermal degradation temperatures. Thus, the 25/70/5 SR/FKM/ FVP blend exhibited higher thermal stability than did the other blend samples due to rubber–filler interactions.

Table VI. Thermomechanical Properties of the SR/FKM/FVP Blends

SR/FKM/FVP	Temperature for tan δ_{max} (°C, from DMA)	
25/75/0	−60.49[a]	−12.71[b]
25/70/5	−57.03[a]	−1.83[b]
25/65/10	−61.51[a]	−2.35[b]
25/55/20	−48.47[a]	−1.82[b]
25/35/40	−48.92[a]	−1.74[b]

[a]SR transition, [b]FKM transition.

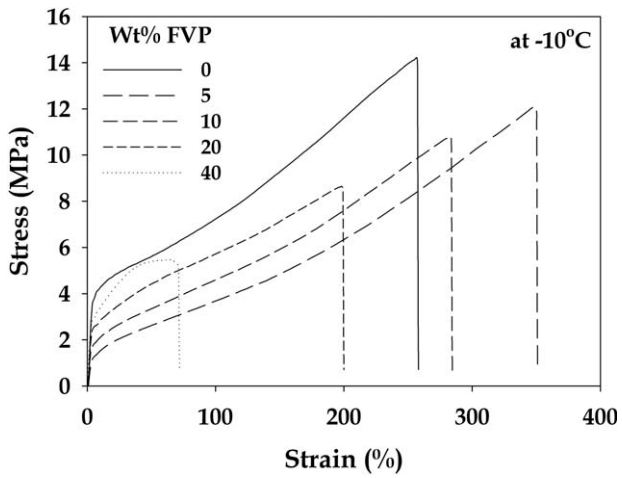

Figure 7. Stress–strain plots of the SR/FKM/FVP blends at –10°C.

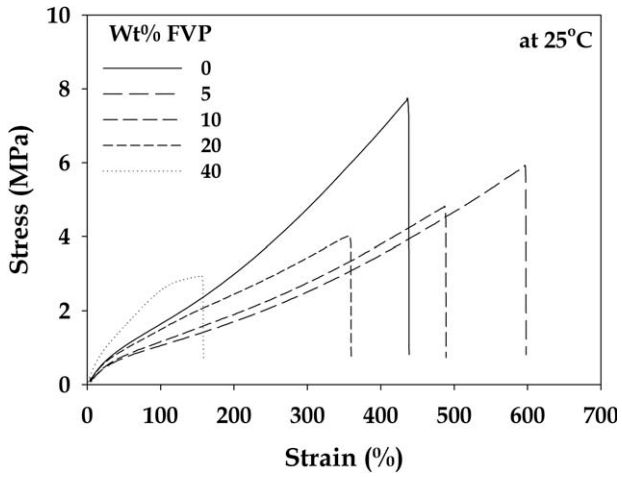

Figure 8. Stress–strain plots of the SR/FKM/FVP blends at 25°C.

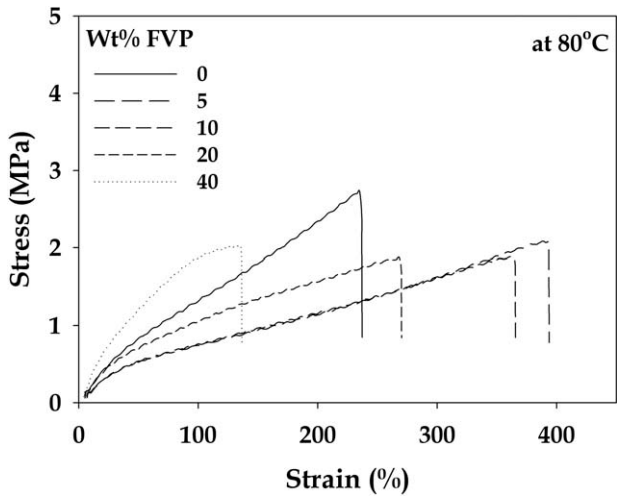

Figure 9. Stress–strain plots of the SR/FKM/FVP blend at 80°C.

Table VII. Physical Properties of Blends

SR/FKM/FVP	Tensile strength (MPa)	Elongation at break (%)
25/75/0	14.2[a] (7.7[b], 2.7[c])	257[a] (437[b], 235[c])
25/70/5	12.1[a] (5.9[b], 2.1[c])	349[a] (597[b], 390[c])
25/65/10	10.8[a] (4.8[b], 1.9[c])	283[a] (487[b], 362[c])
25/55/20	8.6[a] (4.0[b], 1.9[c])	197[a] (358[b], 268[c])
25/35/40	5.5[a] (2.9[b], 2.0[c])	64[a] (155[b], 134[c])

[a]Tensile strength (MPa) and elongation at break (%) at −10°C, [b]Tensile strength (MPa) and elongation at break (%) at 25°C, [c]Tensile strength (MPa) and elongation at break (%) at 80°C.

In Figure 3, DTG curves of the 0, 5, 10, 20, and 40 FVP wt% exhibited a two-step thermal degradation. The first maximum decomposition region of them occurred at 431, 453, 439, 436, and 431°C, respectively and the weight loss of them exhibited 17.7, 19.5, 15.5, 15.0, and 13.5 wt%, respectively. The second region of them occurred at 475, 507, 504, 498, and 489°C, respectively and the weight loss of them exhibited 66.6, 75.9, 75.9, 65.8, and 53.9 wt%, respectively.

The two stages of thermal degradation observed in the SR/FKM/FVP blends are also reflected in the DTG curves shown in Figure 3. The DTG values of SR phase in Figure 3 are 431, 453, 439, 436, and 431°C, respectively. The DTG values of FKM phase in Figure 3 were 475, 507, 504, 498, and 489°C, respectively. The introduction of FVP enhanced the thermal stabilities of the SR/FKM blends.

The temperatures required to result in 1 and 50% weight losses and the percentage weight loss for the second thermal degradation are summarized in Table V. Degradation was initiated earlier in the SR/FKM blend than in the SR/FKM/FVP blends. Similar behavior has been observed in many miscible blends in which one of the components is more prone to degradation than are the others.[27]

DMA Analysis

Dynamic mechanical analysis (DMA) is a versatile and sensitive tool enabling complete exploration of relaxation mechanisms in viscoelastic materials, especially polymer blends. The most common use of DMA is the determination of the glass-transition temperature (T_g), at which the molecular chains of a polymer obtain sufficient energy, usually from thermal sources, to overcome the energy barriers for segmental motion. The storage modulus (E') and loss factors (tan δ) of all the samples are illustrated in Figures 4–6. The magnitude and nature of the change in the dynamic modulus of elasticity are determined by

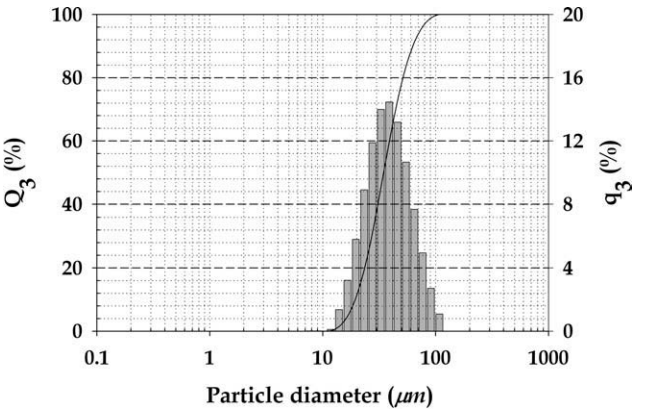

Figure 10. The particle size distribution of FVP.

intermolecular interactions. The latter has a greater influence in the different physical state of the polymer.[28]

Figure 4 illustrates that the storage modulus of the SR/FKM blend was enhanced with the addition of 20 wt% FVP, and that E' increased with increasing FVP content. This improvement in the E' value is due to the high modulus of the FVP phase. In polymer blends, DMA shows a single transition between the individual values of T_g if the two components are fully miscible and only one phase exists.

On the contrary, if the two polymers are immiscible and two distinct phases exist, then the blends will show two distinct peaks. If the polymer blends are partially compatible, their T_g values will shift toward each other.[27] Figure 6 shows the tan δ temperature curves of the SR/FKM/FVP blends. The SR/FKM blend had two glass-transition temperatures of −60 and −12°C. The SR/FKM/FVP blends showed two transitions at −61 to −48°C and −2 to −1°C, which indicates the immiscibility of the two components with these blend ratios. The other two blends showed two peaks, with the main peak due to the FKM and the shoulder due to SR.

Both peaks were shifted toward each other with respect to the individual T_g. This indicates partial miscibility of the 25/70/5 SR/FKM/FVP and 25/65/10 SR/FKM/FVP blends. The peak temperature values are listed in Table VI.

Physical Properties

In order to investigate the elastic-deformation behavior of the SR/FKM/FVP blends, they were investigated at different temperature.

Effects of the blend ratios on the physical properties of the SR/FKM/FVP blends were shown in Figures 7–9, and their physical properties were summarized in Table VII.

Table VIII. Analysis of Particle Size Distribution of FVP

Sample	Particle size distribution (micrometer)					Specific surface area (m^2 cm^{-3})	Rosin Rammler-N
	X_{10}[a]	X_{50}[b]	X_{90}[c]	X_{top}	d_{vm}[d]		
FVP	19.43	34.64	62.69	108.01	41.75	0.189	3.4023

[a]X_{10} is 10% diameters at cumulative distribution volume standard under volume, [b]X_{50} is 50% diameters at cumulative distribution volume standard under volume, [c]X_{90} is 90% diameters at cumulative distribution volume standard under volume, [d]d_{vm} is the mean particle diameter.

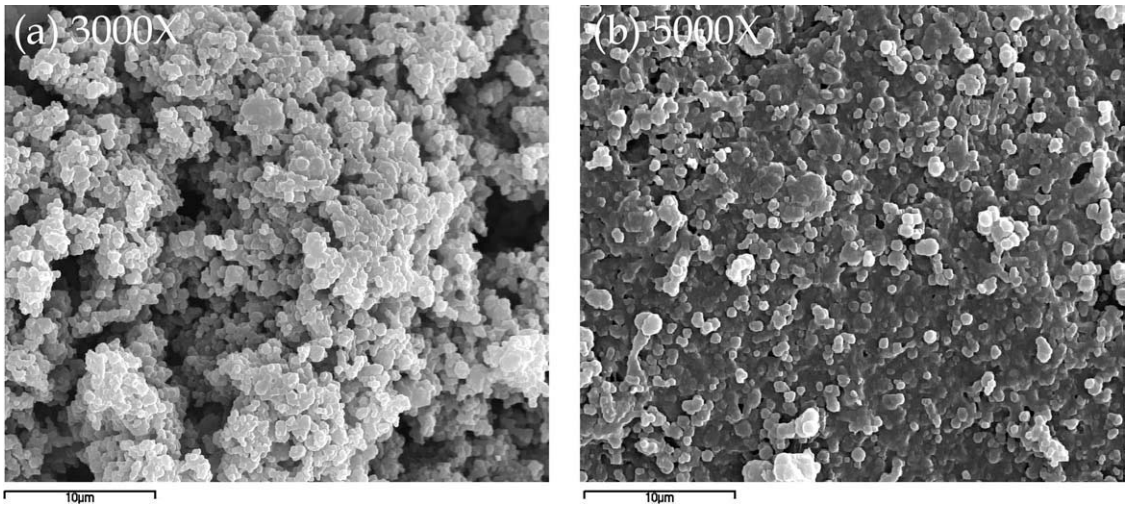

Figure 11. FE-SEM micrographs of fluororubber vulcanizate powder (FVP): (a) ×3000. (b) ×5000.

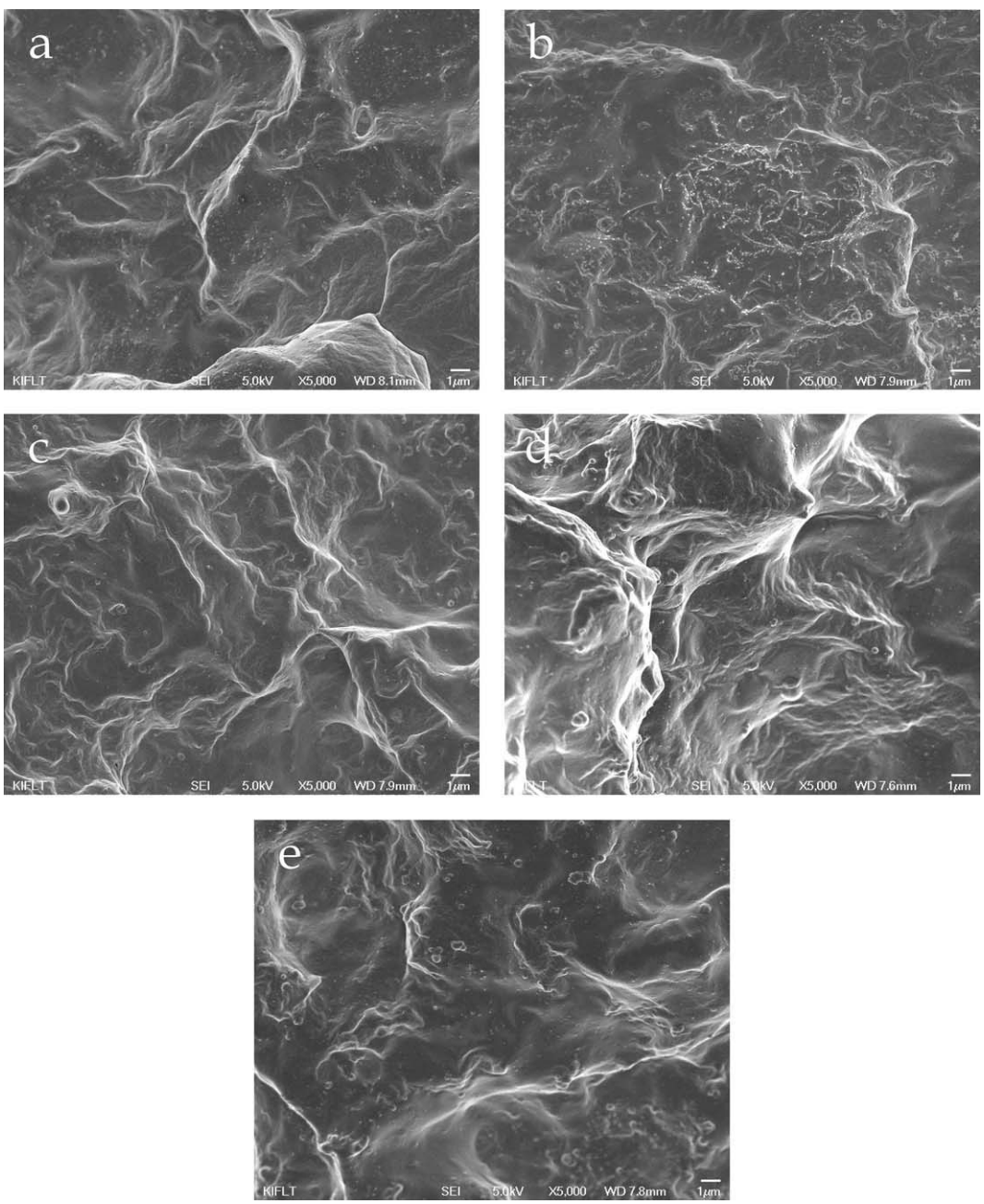

Figure 12. FE-SEM micrographs of the SR/FKM/FVP blends: (a) 25/75/0. (b) 25/70/5. (c) 25/65/10. (d) 25/55/20. (e) 25/35/40.

The modulus decreased and the tensile strength increased in the 5 and 10 wt% FVP blends. In the SR/ FKM/FVP blends, very typical elastic-deformation behavior was observed in 5 and 10 wt% FVP, while the rubber property in the 40 wt% FVP blend disappeared.

Figures 7 and 8 show the physical properties of the SR/FKM/FVP blends at −10 and 25°C, respectively. The tensile strength of the SR/ FKM/FVP blends decreased with the addition of up to 40 wt% FVP. The elongation at break increased with the addition of up to 10 wt% FVP and then decreased thereafter.

Figure 9 shows the physical properties of the SR/FKM/FVP blends at 80°C. The tensile strengths of the SR/FKM/FVP blends decreased with the addition of up to 40 wt% FVP. The elongations at break of the blends also increased with the addition of up to 20 wt% FVP and then decreased.

Particle Size Analysis

The particle size distribution of FVP is shown in Figure 10, and the analysis results are shown in Table VIII. We measured the particle size, the volume standard particle means diameter (d_{vm}), the specific surface area (S_v), and other physical properties related to the particle number, n, according to the Rosin-Rammler distribution. The volume standard particle mean diameter (d_{vm}) was determined using the following equation[29]:

$$d_{vm} = \frac{\sum_i d_i \times \Delta\Phi_i}{100}. \quad (2)$$

where d_{vm} is the mean particle diameter, d_i is a channel of the particle diameter, and $\Delta\Phi_i$ is the volume standard under the volume frequency distribution (% μm^{-1}). In eq. (2), d_i and $\Delta\Phi_i$ denote the particle mean diameter and the percentage of volume existing in the ith channel in the range of 0.1−1000 μm with 55 channels, respectively. After cryogenic grinding, the mean particle diameter (d_{vm}) was 41.75 μm, the maximum particle size (X_{top}) was 108.01 μm, and the minimum particle size was 11.79 μm.

Sizes and Shapes of Vulcanizate Powder Particles

FE-SEM micrographs 3of FVP are shown in Figure 11. The main differences between cryogenically ground rubber powder and material ground in the rubbery state were observed in the surface structure. The cryogenically ground material had a very smooth, glass-like surface.[30] In contrast, as shown in Figure 11, the ground powder consisted of aggregate structures in granule form. FVP consists of a mixture of large particles that are irregular in shape and vary in size from 10 to 100 μm. The smaller particles occur in highly aggregated states. Granules tend to agglomerate after grinding due to tackiness. The powder aggregates break down into mostly spherical particles when they are blended with rubbers.

Morphological Properties

Figure 12(a–e) shows FE-SEM micrographs of the SR/FKM/FVP blends. The SR/FKM blends were homogeneously mixed. FVP was observed to break down into particles with sizes of 1−10 μm during blending with the SR/FKM blend. The SR/FKM/FVP blends showed comparatively smooth surfaces with dispersed particles. The FE-SEM micrographs of the SR/FKM/FVP blends did not significantly change in appearance with increasing FVP content. The domain size of FVP was observed to decrease in Figure 12(b–d). Therefore, FVP recycling is possible.

CONCLUSIONS

With increase of FVP content, the rheometer torque of the SR/FKM/FVP blends increased. The rheometer torque of the 25/35/40 SR/FKM/FVP blend was higher than that of the 25/75/SR/FKM blend.

In the TGA and DTG curves of the SR/FKM/FVP blends, SR/FKM blend exhibited two stages of thermal degradation. With increase in FVP content, the onset degradation temperature also increased, while the onset degradation temperature of the SR/FKM blend decreased. We believe that the onset degradation temperature is controlled by the effects of MT carbon black content in FVP. The DTG curves indicated high degradation temperatures for the 5 wt% FVP blend. However, in more than 5 wt% FVP, the DTG curves indicated a lower onset degradation temperature than those for the other samples. Thus, the 25/70/5 SR/FKM/FVP blend was the most stable due to its higher degradation temperature.

The storage modulus (E') and loss modulus (E'') of the SR/FKM/FVP blends increased with increasing FVP content. These increases in the E' and E'' were due to the high modulus of the FVP phase. The SR/FKM/FVP blends showed only two transitions. The behaviors of the blends indicated the immiscibility of the two components.

The physical properties of the SR/FKM/FVP blends showed very typical elastic-deformation behavior by adding 5 and 10 wt% FVP into the SR/ FKM blends. In the physical properties observed at −10 and 25°C, the tensile strengths of the SR/FKM/FVP blends decreased with increasing FVP content. The elongations at break of the blends increased with the addition of up to 10 wt% FVP and then decreased. This same tendency was observed at 80°C. It is concluded that the replacement of up to 10 wt% FVP is possible without a significant reduction in the physical properties.

Cryogenically ground FVP exists in a highly aggregated state. The particle size distribution was broad, ranging from 10 to 100 μm with an average particle size of 41.75 μm. Ground powder exists as aggregated structures of granules. Cryogenically ground material has a very smooth, glass-like surface.[30] In contrast, cryogenically ground FVP exists in a granular state.

In conclusion, it is possible to recycle FKM in the form of FVP for utilization in SR/FKM/FVP blends. Using SR/FKM/FVP blends, it is possible to replace up to 10 wt% FVP with virgin FKM. To achieve successful rubber recycling, the physical properties that result from the recycling process must be considered.

REFERENCES

1. Isayev, A. I. Rubber recycling, in Rubber Technologist's Hand- book, De, S. K.; White, J. R. Eds.; Rapra Technology Ltd., Shawbury, Shropshire, U. K, **2001;** p 511.
2. De, S. K. *Prog. Rubber Plast. Technol.* **2001,** *17*, 113.

3. Anonymous, Goodyear Tire and Rubber Co., Akron, USA, *Res. Discl* **1975,** *136*, 21.
4. Grebekina, Z. I.; Zakharov, N. D.; Makarov, V. M. *Izv. Vyssh. Uchebm. Zaved, Khim Khim Technol.* **1980,** *23*, 1161.
5. Luo, T.; Isayev, A. I. *J. Elast. Plat.* **1998,** *50*, 133.
6. Adam, G.; Sebenik, A.; Osredkar, U.; Fbnogajee, F.; Veksli, Z. *Rubber Chem. Technol.* **1991,** *64*, 133.
7. Jacob, C.; De, P. P.; Bhowmick, A. K.; De, S. K. *J. Appl. Polym. Sci.* **2001,** *82*, 3293.
8. Fesus, E. M.; Eggleton, R. W. Recyling Rubber Products Sensibly in Rubber World, Rohrer, J., Ed.; Lippincott, J. H: Lippincott & Peto Inc. March, **1991;** Vol. *23.*
9. Dierkers, I. W. Solution to the Rubber Waste Problem Incorating the Use of Recycled Rubber in Rubber World, Rohrer, J., Ed.; Lippincott, J. H: Lippincott & Peto Inc. May, **1996; Vol.** *25.*
10. Suma, N.; Rani, J. *Int. J. Polym. Mater.* **1993,** *21*, 127.
11. Aziz, Y.; Amu, A. *Kautschuk Gummi Kunststoffe* **1992,** *45*, 862.
12. Rajalingam, P.; Baker, W. E. *Rubber Chem. Technol.* **1992,** *65*, 908.
13. Rajalingam, P.; Sharpe, J.; Baker, W. E. *Rubber Chem. Technol.* **1993,** *66*, 664.
14. Pramanik, P. K.; Baker, W. E. *Plast. Rubber Compos Process Process Appl.* **1995,** *24*, 229.
15. Oliphant, K.; Baker, W. E. *Polym. Eng. Sci.* **1993,** *33.* 166.
16. Diao, B.; Isayev, A. I.; Levin, V. Y. *Rubber Chem. Technol.* **1999,** *72*, 152.
17. Ghosh, A.; Antony, P.; Bhattacharya, A. K., Bhowmick, A. K.; De, S. K. *J. Appl. Polym. Sci.* **2001,** *82*, 2326.
18. Ghosh, A.; Kumar, B.; Bhattacharya, A. K.; De, S. K. *J. Appl. Polym. Sci.* **2003,** *88*, 2377.
19. Cho, D. W.; Yoon, C. H. *J. Kor Inst. Rubber Ind.* **1992,** *27*, 275.
20. Sau, K. P.; Chaki, T. K.; Khastgir, D. *J. Appl. Polym. Sci.* **1999,** *71*, 887.
21. Ghosh, A. K.; Maiti, S.; Adhikari, B.; Ray, G. S.; Mustafi, S. K. *J. Appl. Polym. Sci.* **1997,** *66*, 683.
22. Stickney, P. B.; Falb, R. D. *Rubber Chem. Technol.* **1964,** *37*, 1299.
23. Kraus, G. *Adv. Polym. Sci.* **1971,** *8*, 155.
24. Blow, C. M. *Polymer* **1973,** *14*, 309.
25. Dannberg, E. M. *Rubber Chem. Technol.* **1986,** *59*, 512.
26. Wolff, S.; Wang, M.J.; Tan, E.H. *Rubber Chem. Technol.* **1993,** *66*, 163.
27. Paul, D. R.; Newman, S. Polymer Blends; Academic: New York, **1978,** *1*, 141.
28. Iperepechko, I. Acoustic Methods of Investigating Polymers; Mir: Moscow, **1975.**
29. Bilgili, E. *Powder Technol.* **2001,** *115*, 265.
30. Sadhan, K. De.; Avraam I. Isayev.; Klementina, K. *Rubber Recycling* **2005,** *3*, 132.